High Q Factor and High Power Density Ultraviolet Resonant-Cavity Light-Emitting Diodes

Yu-Kun Wang, Bing An, Zhong-Ming Zheng, Wei Ou, Tao Yang, Peng Gu, Yang Mei, Lei-Ying Ying, Jing Yang, De-Gang Zhao, Feng Liang, and Bao-Ping Zhang

***Abstract*— In this work, we fabricated high-performance GaN-based ultraviolet resonant cavity light-emitting diodes (RCLEDs) with dual dielectric distributed Bragg reflectors (DBRs). The devices were configured a copper plate and AlN current confinement aperture, which improved thermal dissipation and increased the maximum output power density up to 84.03 W/cm^2 at injected current density of ∼36 kA/cm^2. The emission wavelength of the devices is 376.7 nm and narrow cavity modes were observed with a linewidth of 0.24 nm, corresponding to a high quality factor (Q) of 1570.**

***Index Terms*— Resonant cavity light-emitting diode, ultraviolet, electroplated copper plate, high Q factor, high power density.**

I. Introduction

THE structure of resonant cavity light-emitting diodes (RCLEDs) includes a planar Fabry–Pérot (FP) cavity consisting of a pair of mirrors at both cavity ends, which usually use metal mirror, epitaxially grown nitride distributed Bragg reflectors (DBRs), and oxide-based DBRs (e.g., SiO_2/TiO_2) [3], [4], [5], [6]. As an intermediate device-between light-emitting diodes (LEDs) and vertical-cavity surface-emitting lasers (VCSELs), RCLEDs combines some of their advantages, such as narrow linewidth, good directivity, and high brightness [1], [2].

For RCLEDs, narrow linewidth and good directivity favor free-space modulation speed and free-space data transmission rate [8]. It can improve the color gamut for display applications, and can also imply superior efficacy in medical applications. For example, narrowband phototherapy with fluorescent bulbs emitting in near UV (nUV) spectral region has become an efficacious method for skin disease and phytochemicals while minimizing the adverse side effects on neighboring normal tissues [3], [4]. The replace of fluorescent bulbs with an UV RCLED with high brightness can simplify the system and reduce the cost greatly.

The Q factor is an important parameter for RCLEDs to realize a narrow emission spectrum. It is defined as the totally stored energy divided by the energy loss over one radian of the oscillating cycle (2π radian), and can be used to evaluate the quality of the resonators [5], [6]. Resonant cavities with a high Q factor can strongly confine photons in small volumes and enhance the light-matter interaction. Hence, for optoelectronic devices, optical resonators with high quality, or equivalently, a high Q factor, are required.

III nitride-based semiconductors, including GaN, AlN, InN, and their alloys, are featured with a large bandgap and a tunable emission wavelength, which can cover the range from the ultraviolet (UV) to the entire visible range. In addition, GaN-based materials have high oscillator strength (typically 10 times higher than GaAs) and large exciton binding energy [7]. These properties suggest that a GaN-based micro cavity with a high Q factor is an ideal platform for RCLEDs.

To date, there have been many reports on GaN-based RCLEDs with high Q-factor and high output power (density), especially in the visible region. Hu et al. realized a 450.6 nm RCLED with a high Q factor of 1720 by placing the ITO layer precisely in the node of the optical field to reduce the absorption of ITO. They further smoothed the surface to reduce optical scattering loss after removing the substrate by using the chemical mechanical polishing (CMP) process and achieved a higher Q value of 2170 [8]. Mei et al. fabricated a green RCLED with a Q value of 6039, which have highly reflective DBRs, low optical scattering loss, and low lateral optical leakage caused by the lateral optical confinement structure (LOC) [9]. Yeh et al. also fabricated a RCLED with an output power density of 116 W/cm^2 at 428 nm using a silicon diffusion defined confinement structure [10].

In the UV field, however, there is limited work on RCLEDs. UV light has many applications in industry, chemistry, materials and medicine such as photocatalytic water purification and sterilization, material lithography, material curing, and medical treatment of skin cancer and psoriasis [3], [4], [11].

Manuscript received 6 May 2024; revised 25 June 2024; accepted 29 June 2024. Date of publication 9 July 2024; date of current version 16 July 2024. This work was supported in part by the National Natural Science Foundation of China under Grant 62234011, Grant U21A20493, and Grant 62104204; in part by the President's Foundation of Xiamen University under Grant 20720220108; and in part by the Natural Science Foundation of the Fujian Province of China under Grant 2023J05020. *(Corresponding authors: Feng Liang; Bao-Ping Zhang.)*

Yu-Kun Wang, Bing An, Zhong-Ming Zheng, Wei Ou, Tao Yang, Peng Gu, Yang Mei, and Lei-Ying Ying are with the Laboratory of Micro/Nano-Optoelectronics, Department of Microelectronics and Integrated Circuit, School of Electronic Science and Engineering, Xiamen University, Xiamen 361005, China (e-mail: wangyukun2@stu.xmu.edu.cn).

Feng Liang, Jing Yang, and De-Gang Zhao are with the State Key Laboratory on Integrated Optoelectronics, Institute of Semiconductors, Chinese Academy of Sciences, Beijing 100083, China (e-mail: liangfeng13@semi.ac.cn).

Bao-Ping Zhang is with the Laboratory of Micro/Nano-Optoelectronics, Department of Microelectronics and Integrated Circuits, Xiamen University, Xiamen 361005, China, and also with the Institute of Nanoscience and Applications, Southern University of Science and Technology, Shenzhen 518055, China (e-mail: bzhang@xmu.edu.cn).

Color versions of one or more figures in this letter are available at https://doi.org/10.1109/LPT.2024.3425535.

Digital Object Identifier 10.1109/LPT.2024.3425535

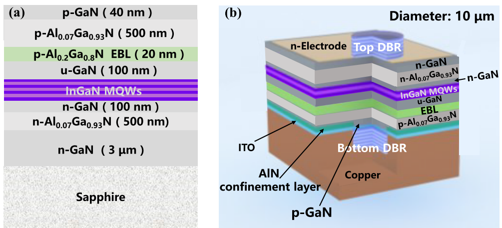

Fig. 1. (a) Schematic structure of the epitaxial wafer. (b) Schematic structure of UVA RCLED.

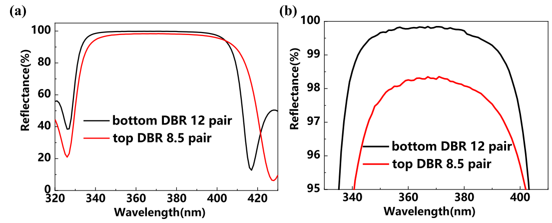

Fig. 2. Reflectance spectra of the top and bottom DBRs of the UVA RCLED from 300-445 nm. (b) Stopband of the top and bottom DBRs.

Moudakir et al. fabricated a 390 nm InGaN-based RCLED, using a Ta_2O_5/SiO_2 DBR and an Ag mirror, and achieved an output power density of 6.68 W/cm^2 [12]. Ji et al. demonstrated a 371.4 nm RCLED with a linewidth of 5.1 nm by introducing a current confinement structure [13]. Compared with visible range, the Q factor of UV RCLEDs is much smaller due to the increased difficulty in fabricating higher reflectivity DBRs in the UV region, the stronger absorption of the commonly used transparent conductive layer indium tin oxide (ITO), the stronger absorption of GaN layers, the higher scattering losses caused by the rough surface after substrate removal [14] and the inferior crystal quality.

In this work, we fabricated GaN-based UVA RCLEDs with a dual dielectric DBR structure, demonstrating exceptional performance with high Q factor and high output power density. Due to the high reflectivity (R $>$ 98%) of the DBRs and the low-loss resonant cavity, the emission of the devices has a narrow linewidth of only 0.24 nm and a high Q value of 1570. Since the thermal dissipation of the UVA RCLEDs was improved by utilizing an electroplated copper substrate and an AlN confinement layer with high thermal conductivity ($\sim$400 and $\sim$200 W/mK, respectively) [1], the mode wavelength showed a slight red shifted with a slope of $\sim$0.2 meV/K and the light output power density reaches 84.03 W/cm^2 at 36 kA/cm^2, corresponding to the thermal roll-over current density. We also investigated the effect of temperature on the Q factor and its underlying causes through temperature-dependent EL testing. These results show that the performance of the UVA RCLEDs has been greatly improved.

II. Material and Methods

Figure 1(a) shows the schematic structure of the epitaxial wafer. The epitaxial layers were grown on a (0001) c-plane sapphire substrate by metal-organic chemical vapor deposition (MOCVD). A thick n-GaN layer was grown on the sapphire substrate. Then, a 500 nm n-type $Al_{0.07}Ga_{0.93}N$ cladding layer (CL), a 100 nm n-GaN layer, $In_{0.05}Ga_{0.95}N$/GaN multi-quantum wells (MQWs), a 100 nm unintentional doped GaN layer, a 20 nm p-$Al_{0.2}Ga_{0.8}N$ electron barrier layer (EBL), a 500 nm n-$Al_{0.07}Ga_{0.93}N$ CL, and a 40 nm p-GaN contact layer were grown.

The schematic structure of UVA RCLEDs is shown in Figure 1(b). The structure consists of a dual dielectric DBR structure (HfO_2/SiO_2) together with an electroplated copper substrate and an AlN lateral optical confinement (LOC) layer. ITO was used as the current spreading layer. In particular, the AlN layer not only dissipated a large amount of heat but also confined photons and electrons [1], [15], [16].

Detailed fabrication of UVA RCLEDs was also described in our previous work [9], [15], [17]. Firstly, a p-GaN mesa with a height of $\sim$30 nm and a diameter of 10 μm was fabricated on the p-GaN surface by dry etching. Then, the deposition of the AlN layer is performed within the etched regions surrounding the mesa, which served as an optical and current confinement structure, due to its lower refractive index than GaN [16] and higher thermal conductivity than SiO_2 [1]. The 30 nm-thick ITO layer was deposited on the wafer surface to improve current spreading, followed by the bottom dielectric DBR and Cr/Au deposition. The 30 nm thickness of ITO layer corresponds to a measured sheet resistance of 19.3 Ω. Then, the copper substrate was fabricated by electroplating on the Cr/Au layer, and the sapphire substrate was removed by a laser lift-off (LLO) process. After the LLO process, we applied the CMP process to reduce the roughness and obtain a smooth n-GaN surface with an RMS value of only 0.22 nm, which reduces optical scattering losses. And the cavity length difference can be controlled within 200 nm across the sample by optimization the CMP process in this study. The devices were separated by inductively coupled plasma (ICP) etching. Finally, a Cr/Au n-electrode and top dielectric DBR were deposited.

III. Results and Discussion

The reflectance spectra of the bottom and top DBRs are illustrated in Figure 2(a). The central wavelength (λc) of the stop band was 372 nm. The bottom DBR and top DBR have diameters of 20 μm and 40 μm, and contain 12 and 8.5 pairs of HfO_2/SiO_2, respectively. The reflectivity of the DBR is measured from a reference DBR deposited on a glass substrate, and light was incident from air during measurement. The reflectivity of the top and bottom DBRs is 99.8% and 98.4%. Moreover, the reflectivity was higher than that of the nitride DBR ($\sim$90%) [12], [18]. As shown in Figure 2 (b), the wide stop band of the DBRs (60 and 70 nm, respectively) covers most of the EL spectrum of UVA RCLED, which is shown below.

As shown in Figure 3 (a), the temperature-dependent photoluminescence (TDPL) spectra of the wafer were measured from 3 to 300 K using a pulsed laser of 320 nm with an excitation energy of 1.64 uJ/pulse. Three emission peaks were observed at 355, 362, and 375 nm, corresponding to the emission of the CL layer, the GaN layer, and the InGaN MQWs, respectively. With the increasing temperature, the three peaks

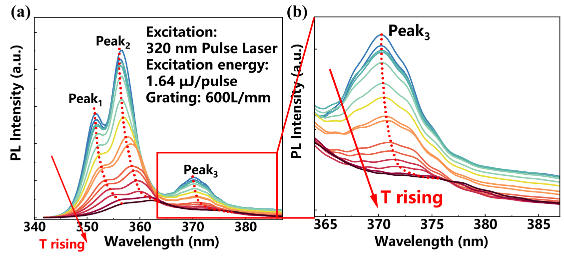

Fig. 3. (a) PL spectra of the epitaxial wafer in the temperature range from 3 to 300 K. (b) The zoom-in image of the 375 nm peak.

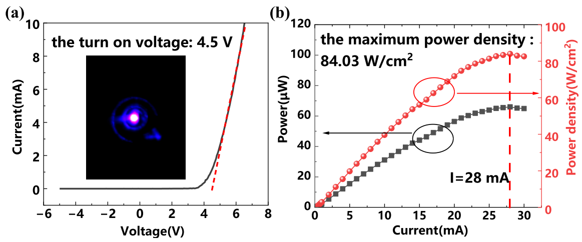

Fig. 4. (a) I-V characteristic of the device (the inset displays the calibrated image to show the emission spot of the device). (b) P-I characteristic of the device.

showed a significant red shift, which can be attributed to the effect of the bandgap shrinking with temperature. Figure 3 (b) shows the zoom-in image of the 375 nm peak. Assume that the internal quantum efficiency (IQE) at low temperatures (3 K) is 100%. Then the IQE was calculated to be 46% at 300 K.

Figure 4 show the current-voltage (I-V) and output power (density)-current (P-I) characteristics of a UVA RCLED with a 10 μm confinement aperture measured at room temperature (RT). As can be seen in Figure 4 (a), the turn-on voltage of the device is 4.5 V, which is a low value for UV RCLEDs [12], [13], indicating that the device has low on-resistance. Additionally, the inset image is the calibrated emission picture of the device at 5 mA. Figure 4 (b) shows the maximum output power density is up to 84.03 W/cm^2 at 28 mA, which is much larger than that of 390 nm UVA RCLED ($\sim$6.68 W/cm^2) [12] and, to the best of our knowledge, the highest value in GaN-based UVA RCLEDs.

Figures 5 (a) and (b) show the electroluminescence spectrum (EL) of the device before deposition of the top DBR and the high-resolution EL spectrum of a complete UVA RCLED at room temperature and 1.5 mA. As shown in Figure 5(a), the peak wavelength of the device before deposition of the top DBR is 377 nm with a linewidth of 4.2 nm. Figure 5(b) shows that the peak wavelength of the UVA RCLED is 376.77 nm. Two higher-order lateral modes can be recognized and the fundamental mode is characterized by the strongest intensity and a narrow linewidth of 0.24 nm. The Q factor is 1570, which is much higher than that of UV (Q $\sim$ 73) [13] and near-UV (Q $\sim$688) [19] RCLEDs. To our knowledge, this is the highest value for GaN-based UVA RCLEDs. Upon comparing Fig. 3 (b) with 5(a) and 5(b), it is apparent that the linewidth decreases from a dozen nanometers to 4.2 nm before the top DBR deposition, and further decreases to 0.24 nm, reflecting a strong resonant cavity effect. The high Q factor is due to the low loss in the cavity, which is enabled by highly reflective DBRs, flat cavity end faces at the atomic level, and the LOC structure [9].

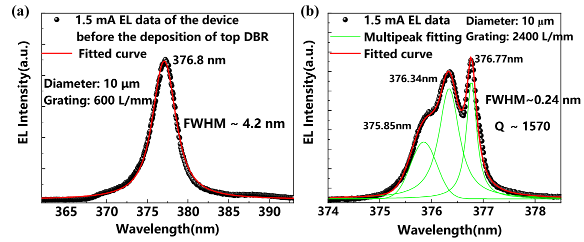

Fig. 5. (a) EL spectrum of the device before the deposition of top DBR. (b) High-resolution spectrum of the 376.77 nm longitudinal mode with a current injection of 1.5 mA at RT.

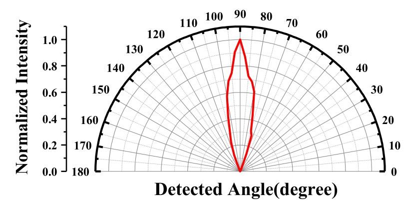

Fig. 6. The divergence characteristics of the fundamental emission mode of a RCLED.

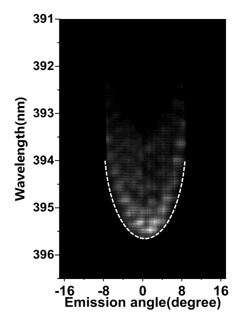

Fig. 7. Emission spectrum of a device with the same structure and a current injection of 1.5 mA at room temperature.

In addition to standard spectral measurement, far-field emission characteristics of the device is also analyzed by using angle-resolved emission measurement. Fig. 6 shows the polar coordinate spectrum of the far-field image of the fundamental emission mode (376.77 nm) of the device. We define the normal direction (90°) as the vertical emission direction of the device. The full-width at half-maximum far-field angle of the fundamental mode is 12.5°. The device exhibits a small divergence angle. Similar phenomenon has been observed in GaAs based RCLEDs [20].

As shown in Fig. 7, we investigated for the distribution of 3D confined optical states in momentum space through angle-resolved measurements by using a device with the same structure. In contrast to the typical parabolic continuous mode dispersion (white dashed line) observed in unconstrained 2D planar microcavities, clear evidence of 3D confined optical states was observed in this study. The far-field mode data formed a parabola, and the dispersion of optical states in k-space split into a series of discrete modes at different energies. The fundamental mode corresponds to the brightest and lowest data point in Fig. 7. These discrete modes represent the manifestation of the 3D confinement effect formed by the AlN aperture confined layer and DBRs [21]. The far-field mode data is highly meaningful for understanding the optical characteristics of UV RCLEDs and selecting specific modes.

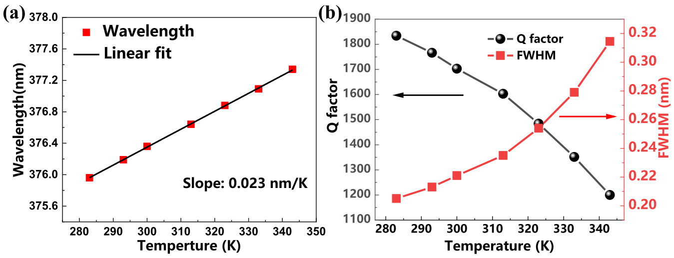

Fig. 8. (a) Wavelength, (b) Q factor and FWHM as a function of device temperature.

Furthermore, we performed temperature-dependent EL measurement from 283 to 343 K to demonstrate the better thermal characteristics of the device at 0.5 mA. The mode wavelength showed a linear red shifted with increasing temperature with a slope of ∼0.20 meV/K, as shown in Figure 8(a). This value is significantly smaller than the 0.32 meV/K [22] and 0.26 meV/K [23] reported in previous studies, demonstrating better thermal characteristics of the device in this study. The Q factor, calculated by the ratio between peak wavelength and FWHM, shows a decrease with increasing temperature, as shown in Fig. 8(b). The Q factor decreases from 1843 at 283 K to 1200 at 343 K.

Previously, the highest power density was 6.68 W/cm^2 at 390 nm [12], and the highest Q value was 73 at 371.4 nm [13]. Compared with previous works, this work has achieved the highest Q value and output power density among UVA RCLEDs. It is believed that our excellent optical and electrical properties are due to the high reflectivity of DBRs, the dual dielectric DBR structure to reduce the growth difficulty of the epilayers, the excellent heat dissipation improved by the AlN and the electroplated copper plate, and the low-loss by a LOC structure, and the good polishing technique to obtain smooth surface after LLO.

IV. Conclusion

In this work, GaN-based UVA RCLEDs have been successfully fabricated with dual dielectric DBR structure, narrow linewidth (0.24 nm) and resonant cavity with high Q value of 1570. By introducing the AlN LOC structure, the current has been effectively confined, and the RCLED has a high injection current density. The electroplated copper substrate and AlN LOC structure improved the heat dissipation capacity of the RCLED, so the devices achieve high power density (84.03 W/cm^2) at high thermal roll-over current density (36 kA/cm^2). Simultaneously, the small redshift coefficient also reflects the excellent heat dissipation capability and good thermal stability of our devices. This work can serve as a reference for the improvement of ultraviolet RCLEDs and the realization of ultraviolet GaN-based VCSELs.

References

[1] Y.-H. Chen et al., “Improvement of thermal dissipation of GaN-based micro cavity light-emitting devices,” *IEEE Photon. Technol. Lett.*, vol. 33, no. 1, pp. 19–22, Jan. 1, 2021, doi: 10.1109/LPT.2020.3040550.

[2] J. A. Tatum, “Evolution of VCSELs,” *Proce. SPIE*, vol. 9001, pp. 78–86, Feb. 2014.

[3] M. A. Khan et al., “13 mW operation of a 295–310 nm AlGaN UV-B LED with a p-AlGaN transparent contact layer for real world applications,” *J. Mater. Chem. C*, vol. 7, no. 1, pp. 143–152, Jan. 2019, doi: 10.1039/c8tc03825b.

[4] F. Benedix, M. Berneburg, and M. Röcken, “Phototherapy with narrow-band vs broadband UVB,” *Acta Dermato-Venereologica*, vol. 85, no. 2, pp. 98–108, Mar. 2005, doi: 10.1080/00015550510025579.

[5] K. J. Vahala, “Optical microcavities,” *Nature*, vol. 424, no. 6950, pp. 839–846, Aug. 2003, doi: 10.1038/nature01939.

[6] Ž. Gačević et al., “Q-factor of (In,Ga)N containing III-nitride microcavity grown by multiple deposition techniques,” *J. Appl. Phys.*, vol. 114, no. 23, pp. 1–7, Dec. 2013, doi: 10.1063/1.4846218.

[7] D. Sanvitto and S. Kéna-Cohen, “The road towards polaritonic devices,” *Nature Mater.*, vol. 15, no. 10, pp. 1061–1073, Oct. 2016, doi: 10.1038/nmat4668.

[8] X.-L. Hu et al., “Fabrication and characterization of high-quality factor GaN-based resonant-cavity blue light-emitting diodes,” *IEEE Photon. Technol. Lett.*, vol. 24, no. 17, pp. 1472–1474, Sep. 1, 2012, doi: 10.1109/LPT.2012.2206110.

[9] Y. Mei, Y.-H. Chen, L.-Y. Ying, Z.-W. Zheng, H. Long, and B.-P. Zhang, “High Q factor electrically injected green micro cavity,” *J. Lightw. Technol.*, vol. 39, no. 9, pp. 2895–2901, May 1, 2021, doi: 10.1109/JLT.2021.3053213.

[10] P. H. S. Yeh et al., “Blue resonant-cavity light-emitting diode with half milliwatt output power,” *Proce. SPIE*, vol. 9768, pp. 65–70, Mar. 2016.

[11] M. Kneissl et al., “Advances in group III-nitride-based deep UV light-emitting diode technology,” *Semicond. Sci. Technol.*, vol. 26, no. 1, Dec. 2010, Art. no. 014036, doi: 10.1088/0268-1242/26/1/014036.

[12] T. Moudakir et al., “Design, fabrication, and characterization of near-milliwatt-power RCLEDs emitting at 390 nm,” *IEEE Photon. J.*, vol. 5, no. 6, Dec. 2013, Art. no. 8400709, doi: 10.1109/JPHOT.2013.2287558.

[13] M.-H. Ji et al., “Growth and characterization of III-N ultraviolet lasers and avalanche photodiodes by MOCVD,” in *Proc. Conf. Lasers Electro-Opt. (CLEO)*, San Jose, CA, USA, May 2017, pp. 1–2, Paper STh1C-3.

[14] Z. Zheng, Y. Li, and O. Paul, “Loss analysis in nitride deep ultraviolet planar cavity,” *J. Nanophotonics*, vol. 12, no. 4, p. 1, May 2018, doi: 10.1117/1.jnp.12.043504.

[15] Y. Mei et al., “A comparative study of thermal characteristics of GaN-based VCSELs with three different typical structures,” *Semicond. Sci. Technol.*, vol. 33, no. 1, Jan. 2018, Art. no. 015016, doi: 10.1088/1361-6641/aa90aa.

[16] S. Hang et al., “On the origin for the hole confinement into apertures for GaN-based VCSELs with buried dielectric insulators,” *Opt. Exp.*, vol. 28, no. 6, p. 8668, Mar. 2020, doi: 10.1364/oe.385787.

[17] R.-B. Xu et al., “Emission dynamics of GaN-based blue resonant-cavity light-emitting diodes,” *J. Lumin.*, vol. 216, Dec. 2019, Art. no. 116717, doi: 10.1016/j.jlumin.2019.116717.

[18] A. R. K. Getty, A. David, Y. Wu, C. Weisbuch, and J. S. Speck, “Demonstration of distributed Bragg reflectors for deep ultraviolet applications,” *Jpn. J. Appl. Phys.*, vol. 46, no. 8L, pp. L767–L769, Aug. 2007, doi: 10.1143/jjap.46.l767.

[19] M. Diagne et al., “Vertical cavity violet light emitting diode incorporating an aluminum gallium nitride distributed Bragg mirror and a tunnel junction,” *Appl. Phys. Lett.*, vol. 79, no. 22, pp. 3720–3722, Nov. 2001, doi: 10.1063/1.1415405.

[20] F. Sarcan, Y. Wang, T. F. Krauss, T. Erucar, and A. Erol, “Dilute nitride resonant-cavity light emitting diode,” *Opt. Laser Technol.*, vol. 122, Feb. 2020, Art. no. 105888, doi: 10.1016/j.optlastec.2019.105888.

[21] G. Dasbach, M. Bayer, M. Schwab, and A. Forchel, “Spatial photon trapping: Tailoring the optical properties of semiconductor microcavities,” *Semicond. Sci. Technol.*, vol. 18, no. 10, pp. S339–S350, Oct. 2003, doi: 10.1088/0268-1242/18/10/308.

[22] K. M. Kelchner et al., “Continuous-wave operation of pure blue AlGaN-cladding-free nonpolar InGaN/GaN laser diodes,” *Appl. Phys. Exp.*, vol. 3, no. 9, Sep. 2010, Art. no. 092103, doi: 10.1143/apex.3.092103.

[23] R. R. Zhuang, P. Cai, and J. L. Huang, “Study the effect of junction temperature on the peak wavelength in GaN-based high-power green light emitting diodes,” *Adv. Mater. Res.*, vols. 399–401, pp. 1034–1038, Nov. 2011, doi: 10.4028/www.scientific.net/amr.399-401.1034.